Accelerated Publications

Identification of a Mn−O−Mn Cluster Vibrational Mode of the Oxygen-Evolving Complex in Photosystem II by Low-Frequency FTIR Spectroscopy†

Hsiu-An Chu, Heather Sackett, and Gerald T. Babcock*

Department of Chemistry, Michigan State University, East Lansing, Michigan 48824

Received July 27, 2000; Revised Manuscript Received October 6, 2000

ABSTRACT: We have developed conditions for recording the low-frequency S_2/S_1 Fourier transform infrared difference spectrum of hydrated PSII samples. By exchanging PSII samples with buffered ^{18}O water, we found that a positive band at 606 cm^{-1} in the S_2/S_1 spectrum in ^{16}O water is clearly downshifted to 596 cm^{-1} in ^{18}O water. By taking double-difference (S_2/S_1 and ^{16}O minus ^{18}O) spectra, we assign the 606 cm^{-1} mode to an S_2 mode and also identify a corresponding S_1 mode at about 625 cm^{-1}. In addition, by Sr and ^{44}Ca substitution experiments, we found that the 606 cm^{-1} mode is upshifted to about 618 cm^{-1} by Sr^{2+} substitution but that this mode is not affected by substitution with the ^{44}Ca isotope. On the basis of these results and also on the basis of studies of Mn model compounds, we assign the 625 cm^{-1} mode in the S_1 state and the 606 cm^{-1} mode in the S_2 state to a Mn−O−Mn cluster vibration of the oxygen-evolving complex (OEC) in PSII. This structure may include additional bridge(s), which could be another oxo, carboxylato(s), or atoms derived from an amino acid side chain. Our results indicate that the bridged oxygen atom shown in this Mn−O−Mn cluster is exchangeable and accessible by water. The downshift in the Mn−O−Mn cluster vibration as manganese is oxidized during the $S_1 \rightarrow S_2$ transition is counterintuitive; we discuss possible origins of this behavior. Our results also indicate that Sr^{2+} substitution in PSII causes a small structural perturbation that affects the bond strength of the Mn−O−Mn cluster in the PSII OEC. This suggests that Sr^{2+}, and by inference, Ca^{2+}, communicates with, but is not integral to, the manganese core.

Photosynthetic water oxidation takes place on the donor side of PSII,[1] which is a multisubunit, integral membrane protein complex (for a review, see ref *1*). Key elements of the OEC are a tetranuclear Mn cluster, Ca and Cl^- cofactors, and a redox active tyrosine residue, Y_Z, with its associated, hydrogen-bonded histidine (D1H190). The OEC accumulates oxidizing equivalents in response to photochemical events within PSII, and cycles through five oxidation states termed S_n ($n = 0-4$), where n denotes the number of oxidizing equivalents stored (*2*, *3*). When the S_4 state is reached, O_2 is released and S_0 is regenerated. The high-resolution X-ray crystal structure of PSII is not yet available, although considerable recent progress has been made (*4*). From extensive EXAFS studies, however, the OEC is suggested to consist of a pair of di-μ-oxo bridged Mn dimers (*5*), but the exact geometry remains a matter of controversy (*6*).

Another potentially important structural technique for studying the OEC is Fourier transform infrared spectroscopy (FTIR). On the basis of studies of Mn model compounds, several diagnostic manganese−ligand and manganese−substrate modes are expected to occur in the low-frequency region (<1000 cm^{-1}) of the IR spectrum (*7*, *8*). For example, Mn_2 di-μ-oxo core vibrations have an intense and characteristic IR absorption around 600−700 cm^{-1}. However, water also absorbs IR radiation strongly in this region, which has limited previous FTIR studies of the OEC to higher frequencies (>1000 cm^{-1}). We have overcome the technical obstacles that have blocked access to the low-frequency region and reported the low-frequency (1000−350 cm^{-1}) S_2/S_1 difference spectra of partial dehydrated PSII samples (*9*−*11*). A recent resonance Raman study of the low-frequency region has made a similar effort to gain access to metal−ligand modes (*12*). In this communication, we use ^{18}O water exchange and Sr and ^{44}Ca reconstitution experiments to identify a Mn−O−Mn cluster vibrational mode in the S_2/S_1 difference spectrum of the PSII OEC. To our knowledge, this is the first report of a low-frequency, metal−ligand vibrational mode in a protein that has been identified by FTIR.

† This work was supported by the USDA Competitive Research Grants Office and by the U.S. Public Health Service (NIH Grant GM 37300).

* To whom correspondence should be addressed: Department of Chemistry, Michigan State University, East Lansing, MI 48824. Telephone: (517) 355-9715, ext 258. Fax: (517) 353-1793. E-mail: Babcock@cem.msu.edu.

[1] Abbreviations: EPR, electron paramagnetic resonance; EXAFS, extended X-ray absorption fine structure; FTIR, Fourier transform infrared spectroscopy; MES, 2-(*N*-morpholino)ethanesulfonic acid; OEC, oxygen-evolving complex; OTG, octyl β-D-thioglucopyranoside; PSII, photosystem II; XAS, X-ray absorption; Y_Z, tyrosine 161D1.

10.1021/bi001751g CCC: $19.00
Published on Web 11/03/2000

MATERIALS AND METHODS

PSII OTG (octyl β-D-thioglucopyranoside) cores, retaining the three extrinsic polypeptides, were prepared from PSII BBY membranes (*13*) as described in ref *14*. Typical oxygen evolution rates for our PSII OTG cores were about 1400 μmol of O_2 (mg of Chl)$^{-1}$ h^{-1} (*10*). Sr- or Ca-reconstituted samples were prepared from 2 M NaCl-washed PSII OTG cores. These cores were washed once with SMN buffer with 1 mM EGTA and then washed twice either with SMN buffer [400 mM sucrose, 15 mM NaCl, and 50 mM Mes (pH 6.0)] with 15 mM $SrCl_2$ or 15 mM $CaCl_2$ for hydrated samples or with FTIR buffer [150 mM sucrose, 5 mM NaCl, and 5 mM Mes (pH 6.0)] with 5 mM $SrCl_2$ or 5 mM $CaCl_2$ for partially dehydrated samples. For ^{44}Ca-reconstituted samples, the buffer contained 150 mM sucrose, 10 mM NaCl, 5 mM $^{44}CaCO_3$, and 5 mM Mes (pH 6.0). $^{44}CaCO_3$ (^{44}Ca, 96.1%) was purchased from Cambridge Isotope Laboratories.

Hydrated samples for FTIR measurements were prepared by spinning down PSII OTG cores (15−30 min at 20 000 rpm) to produce a pellet that was then sandwiched between two AgBr sample windows. For ^{18}O water exchange, the PSII pellet was resuspended in buffered ^{18}O water (SMN, pH 6.0) and then spun down (15−30 min at 20 000 rpm) to obtain the pellet. ^{18}O water (>95%) was purchased from ISOTEC and ISONIC. For S_2/S_1 FTIR measurements of hydrated PSII samples, 2 μL of a fresh 20 mM ferricyanide stock solution was dried on the AgBr sample windows before adding the PSII pellet. Partially dehydrated PSII samples for FTIR measurements were prepared as described in ref *10*. FTIR experiments were performed on a Bomen MB101 spectrometer with a CsI beam splitter and a liquid He-cooled Si bolometer. Samples were cooled to 250 K by using a home-built liquid nitrogen cryostat (*15*). A custom-built, coated CdTe filter was used to limit the FTIR bandwidth and eliminate the HeNe calibration beam (*16*). The sample temperature was regulated to ±0.1 K with a temperature controller (LakeShore 321). Samples were illuminated by a single flash from a frequency-doubled Nd:YAG laser (Quanta-Ray GCR-11) (532 nm, ~7 ns, ~30 mJ pulse^{-1} cm^2). Flash-induced S_2/S_1 FTIR difference spectra were obtained by determining the ratio of the spectra obtained before illumination to those after the flash.

For FTIR measurements in the absence of ferricyanide, because of charge recombination between the acceptor quinone and the manganese cluster at 250 K (the half-time is about 2−3 min under our conditions), spectra were recorded in shorter times (60 scans, about 72 s) compared to the times used for ferricyanide-containing samples (150 scans, about 3 min). After completion of the light spectrum, we waited 20−30 min to let the OEC decay back to the S_1 state, and recycled the same sample (total of three to five times) to improve the signal-to-noise ratio.

RESULTS

We found that water absorbs much less strongly in the 350−650 cm^{-1} region when it is frozen into ice. This IR window becomes wider as the temperature is further decreased to 130 K (the lower limit of our cryostat). By controlling the amount of sample and the water content, we have been able to record the S_2/S_1 difference spectrum by using hydrated PSII samples at 250 K. Figure 1 shows S_2/S_1 difference spectra of hydrated PSII RCC samples in buffered ^{16}O (solid line) or ^{18}O (dotted line) water at 250 K. The ^{16}O spectrum reproduces the S_2/S_1 spectrum of partially dehydrated PSII samples that we reported previously (*9*−*11*). For example, positive bands at 631, 606, and 592 cm^{-1} and negative bands at 618, 577, 498, 488, 411, and 390 cm^{-1} are present in both spectra (compare the solid line in Figure 1 with Figure 4 in ref *11*). The amount of time required for the hydrated samples to reach thermal equilibrium with its surroundings (<1 h) is much shorter than that for partially dehydrated samples (2−3 h); moreover, it is more straightforward to do ^{18}O water exchange with hydrated PSII samples. We found that a positive band at 606 cm^{-1} in the S_2/S_1 spectrum of PSII samples in buffered ^{16}O water (Figure 1, solid line) is very likely downshifted and overlapping with the 592 cm^{-1} mode from ferrocyanide (*10*) upon ^{18}O water exchange (Figure 1, dotted line). The appearance of this ferrocyanide mode at 592 cm^{-1} in the difference spectra indicates that ferricyanide accepts an electron from Q_A^- to become reduced after the flash. The double-difference (^{16}O minus ^{18}O) spectrum is shown as the middle spectrum in Figure 1. The 609/596 cm^{-1} set of difference peaks in the double-difference spectrum provides convincing evidence that we have observed a mode that involves an exchangeable oxygen in its normal coordinate and that this mode shifts upon the $S_1 \rightarrow S_2$ transition.

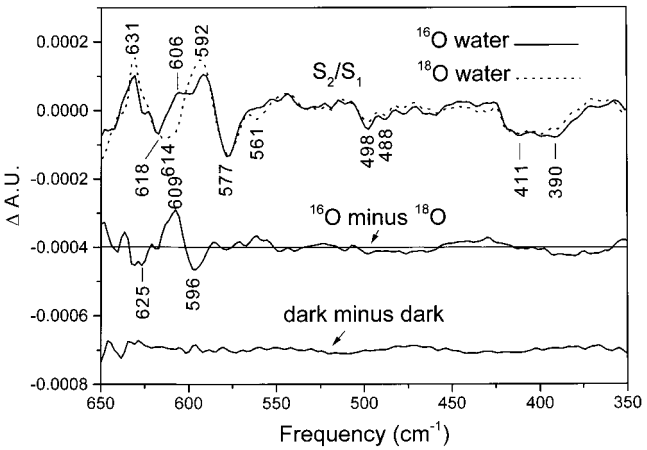

FIGURE 1: Low-frequency S_2/S_1 spectra of hydrated spinach PSII RCCs in buffered ^{16}O (solid line, 1050 scans) or ^{18}O (dotted line, 750 scans) at 250 K, in the presence of ferricyanide. The dark minus dark spectrum (750 scans) was collected immediately before the light minus dark spectra of the same samples. The ^{18}O spectrum is normalized to match the overall intensity of ^{18}O insensitive bands in the ^{16}O spectrum. The double-difference (^{16}O minus ^{18}O) spectrum is generated by subtracting the ^{18}O spectrum from the ^{16}O spectrum. All spectra were collected at 4 cm^{-1} resolution.

We had originally adapted the ferri/ferrocyanide technique of Noguchi (*17*) for our low-frequency work because it contributed fewer bands in the low-frequency region than quinones (*9*−*11*). Ironically, the 592 cm^{-1} ferrocyanide mode obscures a critical region of the spectrum. To determine the exact isotopic shift of the 606 cm^{-1} mode without interference from the ferrocyanide band, we recorded the flash-induced FTIR difference spectrum of hydrated PSII samples in the absence of ferricyanide at 250 K (see Figure 2). Under these conditions, the quinones (mostly likely Q_B) accept the electron. The spectral features in the 550−650 cm^{-1} region in Figure 2 are very similar to those in Figure 1, except that the ferrocyanide band at 592 cm^{-1} is absent. Without the

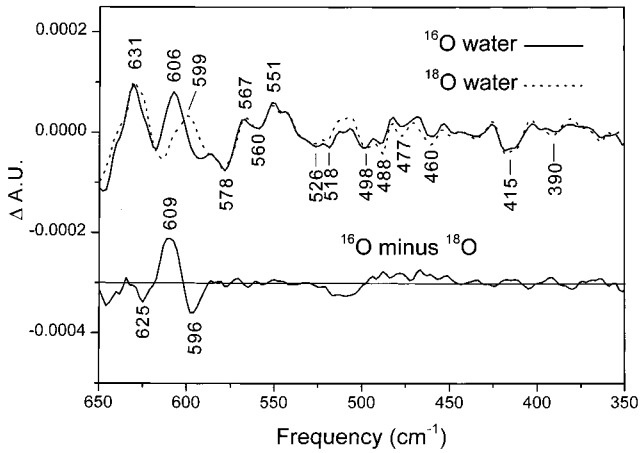

FIGURE 2: Flash-induced FTIR spectra of hydrated spinach PSII RCCs in buffered ^{16}O (solid line, 600 scans) or ^{18}O water (dotted line, 540 scans) at 250 K, in the absence of ferricyanide. The double-difference (^{16}O minus ^{18}O) spectrum is generated in the same way as that shown in Figure 1. All spectra were collected at 4 cm^{-1} resolution.

interference of ferrocyanide, the 606 cm^{-1} mode in the ^{16}O spectrum (Figure 2, top spectrum, solid line) is clearly downshifted to 599 cm^{-1} in the ^{18}O spectrum (Figure 2, top spectrum, dotted line). The double-difference (^{16}O minus ^{18}O) spectrum is shown as the bottom spectrum in Figure 2.

Because the 606 cm^{-1} mode is a positive band in the S_2/S_1 spectrum, it arises as the S_2 state is generated. This suggests that an S_1 mode has been shifted in forming the S_2 state. If this is the case, we expect to see evidence of this in the S_2/S_1 difference spectrum. In the double-difference spectrum of Figure 2, there is a weak negative band at 625 cm^{-1} in addition to the 609/596 cm^{-1} derivative-shape feature that we have discussed thus far. Although the 625 cm^{-1} band is weak, it is clearly above the signal-to-noise ratio and repeats in both the presence (Figure 1) and absence (Figure 2) of ferricyanide.[2] Figure 3 shows a simple model for interpreting these spectral features in the double-difference spectra of Figures 1 and 2. The 606 cm^{-1} mode is predominately an S_2 mode that downshifts to 596 cm^{-1} upon ^{18}O water exchange. The corresponding S_1 mode is present as an adjacent band at about 625 cm^{-1} and becomes negative in the S_2 minus S_1 difference spectrum. This S_1 mode downshifts to about 613 cm^{-1} upon ^{18}O water exchange. In the double-difference spectrum, the S_2 606 cm^{-1} mode in ^{16}O and the S_1 ~613 cm^{-1} mode in ^{18}O are both positive and overlap in the 600−620 cm^{-1} region. Because the intensity of the S_1 mode is much weaker than that of the corresponding S_2 mode at 606 cm^{-1} and also because there is a strongly overlapping but oxygen-isotope-insensitive mode at 631 cm^{-1}, this S_1 mode is apparent only in the double-difference spectra of Figures 1 and 2.

To identify the origin of the 606 cm^{-1} mode and also possible Ca^{2+} modes in the S_2/S_1 spectrum, we substituted natural abundance (^{40}Ca, 96.947%) Ca^{2+} ions in PSII samples with Sr^{2+} and with the ^{44}Ca isotope. Figure 4 shows the S_2/S_1 spectra of Sr^{2+} (solid line)- and Ca^{2+}-reconstituted (dotted line), partially dehydrated PSII RCCs. The double-difference (Ca^{2+} minus Sr^{2+}) spectrum is shown at the bottom. We found that difference vibrational modes in both spectra are very similar except that the 606 cm^{-1} mode in the spectrum of Ca^{2+}-reconstituted samples is most likely upshifted to about 618 cm^{-1} in that of Sr^{2+}-reconstituted samples. Thus, these spectra implicate Ca^{2+} and Sr^{2+} in determining the vibrational characteristics of the 606 cm^{-1} mode.

To test if Ca^{2+} is directly involved in the normal coordinate of the 606 cm^{-1} mode in the S_2/S_1 spectrum or if the Sr substitution causes a structural perturbation to the OEC and affects this mode indirectly, we carried out the $^{44}Ca^{2+}$ substitution experiments shown in Figure 5. If Ca^{2+} is directly involved in the 606 cm^{-1} mode in the S_2/S_1 spectrum, we should see a clear downshift in this mode when natural abundance ^{40}Ca is replaced with the heavier ^{44}Ca isotope. However, Figure 5 shows that the 606 cm^{-1} mode in the $^{40}Ca^{2+}$-reconstituted spectrum (dashed line) is not affected by $^{44}Ca^{2+}$ substitution (solid line). Therefore, we conclude that the 606 cm^{-1} mode in the S_2/S_1 spectrum does not involve Ca^{2+} directly in the normal coordinate. In addition,

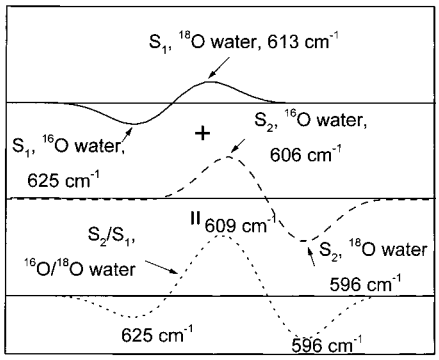

FIGURE 3: Simple model for the spectral features in the double-difference (S_2/S_1 and ^{16}O minus ^{18}O) spectra in Figures 1 and 2. A constructed model of the ^{16}O/^{18}O S_1 spectrum is shown as the top spectrum (solid line). The modeled ^{16}O/^{18}O S_2 spectrum is shown as the middle spectrum (dashed line). The double-difference (S_2/S_1 and ^{16}O minus ^{18}O) spectrum is shown as the bottom spectrum (dotted line). The frequency for each mode listed in the S_1 and S_2 spectra (top and middle) is an approximate (±2 cm^{-1}) number.

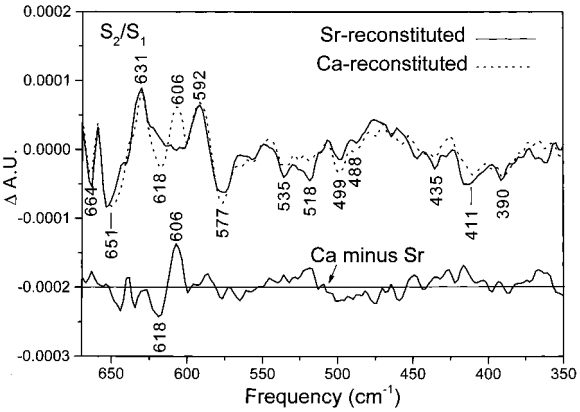

FIGURE 4: Low-frequency S_2/S_1 spectra of partially dehydrated, salt-washed, Sr^{2+}-reconstituted (solid line, 450 scans) or Ca^{2+}-reconstituted (dashed line, 450 scans) spinach PSII RCCs at 250 K in the presence of ferricyanide. The double-difference (Ca minus Sr) spectrum is generated by subtracting the Sr^{2+}-reconstituted spectrum from the Ca^{2+}-reconstituted spectrum. Both spectra were collected at 4 cm^{-1} resolution.

[2] In the region above 635 cm^{-1}, the baseline becomes noisy (see Figure 1, "dark minus dark" spectrum), as the polyethylene windows of our bolometer become progressively opaque and water absorbance becomes significantly stronger. Accordingly, we ignore this frequency region (≥635 cm^{-1}) in our single- and double-difference spectra.

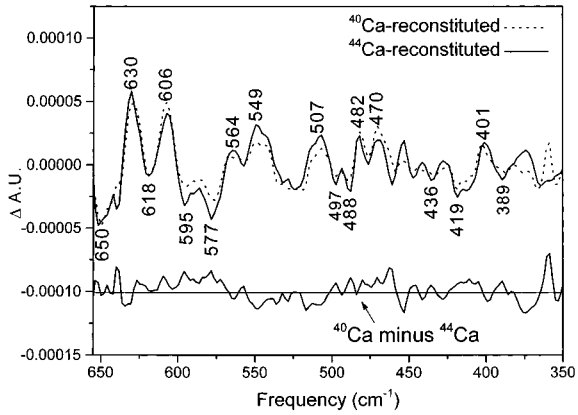

FIGURE 5: Flash-induced FTIR difference spectra of partially dehydrated, salt-washed, $^{40}Ca^{2+}$-reconstituted (dashed line, 600 scans) or $^{44}Ca^{2+}$-reconstituted (solid line, 720 scans) spinach PSII RCCs at 250 K in the absence of ferricyanide. The double-difference ($^{40}Ca^{2+}$ minus $^{44}Ca^{2+}$) spectrum is generated by subtracting the $^{44}Ca^{2+}$-reconstituted spectrum from the $^{40}Ca^{2+}$-reconstituted spectrum. Both spectra were collected at 4 cm^{-1} resolution.

from the double-difference (^{40}Ca minus ^{44}Ca) spectrum of Figure 5, we found no modes in the spectrum that were sensitive to the mass of Ca^{2+}.

DISCUSSION

Our results show that the 606 cm^{-1} mode in the S_2/S_1 spectrum is sensitive to ^{18}O water but not to ^{44}Ca substitution in PSII. Therefore, the origin of this mode is most likely a Mn−oxygen mode of the OEC in which the oxygen exchanges on the ≥30 min time scale in the S_1 state. If the oxygen exchange occurs only when the S_2 state is formed, then the rate of exchange is considerably faster (≤1 min). From studies of inorganic compounds, librational modes of coordinated water and metal−O (H_2O and OH) stretch modes are generally broad and weak (*7*). In addition, IR modes for ν(Mn═O) and ν_{asy}(Mn−O−Mn) for singly oxo-bridged Mn cluster usually occur above 700 cm^{-1} and typically have a 30−40 cm^{-1} ^{18}O downshift (*8*), much larger than the 10−15 cm^{-1} ^{18}O downshift we observed for the 606 cm^{-1} mode. Therefore, they are unlikely to be the origin of the 606 cm^{-1} mode.

Nonetheless, several potential candidates for the origin of the 606 cm^{-1} mode remain. The first is the Mn_2 di-μ-oxo core. By EXAFS and model compound studies, the 2.7 Å vector in EXAFS spectra of the OEC has been assigned to the Mn_2 di-μ-oxo core (*5*). The Mn_2 di-μ-oxo core in Mn model compounds gives rise to a strong and characteristic IR absorption between 600 and 700 cm^{-1} (*7*, *8*). The Mn_2 di-μ-oxo core modes also typically exhibit a 30−40 cm^{-1} downshift caused by double ^{18}O labeling (*8*, *18*). However, single ^{18}O labeling of one of the bridged oxygen atoms in the Mn_2 di-μ-oxo core is expected to give a smaller ^{18}O shift (*19*). For example, an IR study of Mn model compounds with the Mn_2 di-μ-oxo core structure reported a 9 cm^{-1} downshift by exchange with 53% ^{18}O water (*20*). Moreover, the bridging oxygen atoms in Mn_2 di-μ-oxo cores with a (3+, 4+) oxidation state are exchanged with ^{18}O water within 30 min in Mn model compounds (*18*, *21*). From the results presented above, we consider a Mn_2 di-μ-oxo core vibrational mode as a potential candidate for the 606 cm^{-1} mode. The second possibility for the 606 cm^{-1} mode is the ν_{sym}(Mn−O−Mn) mode. In studies of Mn and Fe model compounds, the ν_{sym}(Mn−O−Mn) mode is expected to occur ∼570−350 cm^{-1} and have an ^{18}O shift between 0 and 17 cm^{-1} (*22*, *23*). Therefore, both the frequency and the ^{18}O shift for the ν_{sym}(Mn−O−Mn) mode are close to the 606 cm^{-1} mode that we observe. In addition, one study reported that the bridging oxygen atom in the Mn_2 μ-oxo core is exchanged with ^{18}O water within 15−30 min (*22*). Although the intensity of the ν_{sym}(Mn−O−Mn) mode is expected to be weak in IR, the possibility that the 606 cm^{-1} mode arises from a ν_{sym}(Mn−O−Mn) mode cannot be ruled out. A third potential candidate is the μ_3-O, μ_2-O core in a Mn trimer/monomer structure (distorted cubane). On the basis of EXAFS and EPR results, a Mn trimer/monomer structure has been proposed as one of the potential structural models for the OEC (*21*, *24*−*26*). Unfortunately, up to now, there are no Mn model compounds that closely mimic this proposed structure. Nonetheless, in studies of multinuclear Mn compounds with a μ_3-O bridge(s), Mn μ_3-O core modes occur in the 650−600 cm^{-1} region (*26*, *27*). However, one study (*26*) shows that the exchange rates of the μ_3-O atoms in the symmetric cubane Mn models are much slower (days) than we observed for the 606 cm^{-1} mode (<30 min). It will require further studies of Mn model compounds or an X-ray crystal structure of the PSII OEC to test whether a Mn μ_3-O, μ_2-O core in the Mn trimer/monomer structure provides the 606 cm^{-1} mode.

From the arguments presented above, we assign the 606 cm^{-1} mode to a Mn−O−Mn cluster mode of the OEC in a multiply bridged structure. For the moment, however, we leave open the identity of the other bridging atoms. In addition, our results and the behavior of Mn model compounds also suggest that, if the 606 cm^{-1} mode arises from the Mn_2 di-μ-oxo core structure, only one of the bridged oxygen atoms in the Mn−O−Mn cluster that gives rise to the 606 cm^{-1} mode can be exchanged with water under our experimental conditions. On the other hand, if the 606 cm^{-1} mode arises from the Mn_2 μ_3-O, μ_2-O core of the distorted cubane structure, and if the Mn μ_3-O is indeed exchanged much more slowly than the Mn μ_2-O, this provides an explanation for why only one of the bridged oxygen atoms in the Mn−O−Mn cluster can be exchanged with water under our conditions.

In addition to the S_2 mode at 606 cm^{-1}, we identified a corresponding S_1 mode at ∼625 cm^{-1}. Our result suggests that there is a small decrease in bond strength in the Mn−O−Mn cluster of the OEC upon the S_1-to-S_2 transition. If the 606 cm^{-1} mode arises from the Mn_2 di-μ-oxo core structure, our result seems to contradict a previous IR study on Mn model compounds in which a 6 cm^{-1} upshift of a Mn_2 di-μ-oxo core mode was reported upon oxidation of the Mn_2 (3+, 4+) state to the Mn_2 (4+, 4+) state (*20*). Simple electronic considerations also predict that as the oxidation level increases, the Mn−oxo bonds will contract and lead to an increase in the bond strength of the Mn_2 di-μ-oxo core. However, by studying the crystal structures of Mn model compounds with the Mn_2 di-μ-oxo core structure, Brudvig and co-workers found that the Mn−ligand bond lengths indeed decrease with increased oxidation state, but that the contractions occur mainly in the ancillary Mn−ligand bonds, not in the Mn di-μ-oxo core (*28*). Therefore, the influence

of the valence change on the frequencies of Mn_2 di-μ-oxo core modes is likely to be small. This is further supported by a resonance Raman study that reported a 1 cm^{-1} downshift of a Mn_2 di-μ-oxo core mode upon oxidation of the Mn_2 (3+, 4+) state to the Mn_2 (4+, 4+) state (*18*). It is very likely that other factors [e.g., changes in coordination sphere (ligands and geometry), loss of the Jahn−Teller state, and perturbations to the hydrogen bonds of the OEC] account for the frequency change that we observe for the OEC. In fact, such changes in coordination sphere and hydrogen bonding within the OEC have been suggested to occur upon the S_1-to-S_2 transition (*17*, *29*−*32*).

If the 606 cm^{-1} mode arises from the Mn_2 di-μ-oxo core structure, our results also seem counter to previous XAS studies that showed that there is no significant change in the Mn−Mn distance of the Mn_2 di-μ-oxo cores upon the S_1-to-S_2 transition (*28*). However, by studying Mn models with the Mn_2 di-μ-oxo structure, we found that there are no clear correlations between the frequency of the Mn_2 di-μ-oxo core mode and the Mn−Mn distance. Instead, this mode seems to have a correlation between the frequency of the Mn_2 di-μ-oxo core mode and the ligand types (O vs N ligations) (N. Law and G. T. Babcock, unpublished results). A better understanding of the coordination sphere and hydrogen-bonding status of the PSII OEC in its various S states, which is accessible with FTIR techniques, and a more complete analysis of Mn model compounds will assist in understanding the nature of this frequency change.

Our results on Sr- and ^{44}Ca-reconstituted PSII samples suggest that Sr^{2+} substitution in PSII causes a small structural perturbation by, for example, altering hydrogen bonding or the ligand geometry of the Mn−O−Mn cluster in the PSII OEC. This structural perturbation very likely accounts for the observation of the $g = 2$ modified multiline and the enhanced $g = 4.1$ EPR signals in the S_2 state of Sr-substituted PSII samples (*33*, *34*). An EXAFS study of the S_1 state of the OEC suggested that there is a small but reproducible change in the Mn−Mn distance of a Mn_2 di-μ-oxo core of the OEC upon Sr substitution (*32*). Riggs-Gelasco et al. proposed a hydrogen-bonding interaction between a bound water molecule ligated to Ca (Sr) and a bridged oxygen atom in a Mn_2 di-μ-oxo core of the OEC to account for their EXAFS results (*32*). In addition, several EXAFS studies and one recent solid-state NMR study have suggested that Ca (Sr) is in proximity to the manganese cluster (*5*, *36*−*38*). A possible oxo or carboxylate bridge between Ca (Sr) and the manganese cluster has been proposed (*5*, *17*, *36*−*38*). On the basis of these studies and our results, we conclude that Sr^{2+}, and by inference, Ca^{2+}, communicates with, but is not integral to, the manganese core of the OEC.

A number of structural mechanisms for photosynthetic water oxidation have been proposed (see refs *24*, *30*, *31*, and *39*−*42* for examples). One of the important debates is whether the substrate water binds at terminal or bridged positions of the Mn cluster (*24*, *30*). Another is the geometry of the cluster (*5*, *6*, *21*, *24*, *25*). Even if the "dimer of dimers structure" (*5*), which has been fashionable for almost a decade, turns out to be incorrect, we note, in passing, that this does not invalidate the H atom abstraction model that we have proposed, as long as the O═O bond templating function of two of the Mn is preserved (*30*, *31*). Returning to the terminal versus bridging consideration, we find that our results indicate that the bridged oxygen atom in the Mn−O−Mn cluster that gives rise to the 606 cm^{-1} mode is accessible to and can be exchanged with bulk-phase water. The upper limit for this exchange is that it occurs on the minutes or faster time scale as we find that it is complete within our 30 min time resolution. The time resolution in our experiments is limited by the time needed for spinning down the samples, loading the samples into the spectrometer, cooling to 250 K, and waiting for the sample to equilibrate with the surroundings. Therefore, the proposal that substrate water binds at bridged positions of the Mn cluster is not at odds with the results presented here (*24*). In addition, a recent FTIR study has detected an O−H stretching vibration mode of a water molecule that undergoes a structural change upon the S_1-to-S_2 transition of the OEC (*43*). However, it remains unknown whether this water molecule is a substrate for the OEC. If this water is a substrate molecule and is directly bound to a Mn or Ca ion of the OEC, then ^{18}O sensitive Mn−O or Ca−O stretching and librational modes of this substrate water should occur in our low-frequency S_2/S_1 FTIR difference spectrum. However, we do not yet detect any of these Mn−substrate modes in our low-frequency S_2/S_1 spectra (Figures 1 and 2). On the basis of studies of inorganic compounds with coordinated water (*7*, *44*), we suspect that the intensity of these possible metal−hydrate modes is likely to be too weak ($\Delta A \leq 3 \times 10^{-5}$) to be identified under our current experimental conditions. We are working now to further improve the signal-to-noise ratio in our spectra to identify these putative metal−hydrate modes. Their frequencies and exchangeabilities will provide an incisive test for current models of O_2 evolution.

ACKNOWLEDGMENT

We thank Drs. Takumi Noguchi, Warwick Hillier, and Neil Law for helpful discussion.

REFERENCES

1. Debus, R. J. (2000) *Met. Ions Biol. Syst. 37*, 657−711.
2. Joliot, P., Barbieri, G., and Chabaud, R. (1969) *Photochem. Photobiol. 10*, 309−329.
3. Kok, B., Forbush, B., and McGloin, M. (1970) *Photochem. Photobiol. 11*, 457−475.
4. Zouni, A., Jordan, R., Schlodder, E., Fromme, P., and Witt, H. T. (2000*) Biochim. Biophys. Acta 1457*, 103−105.
5. Yachandra, V. K., Derose, V. J., Latimer, M. J., Mukerji, I., Sauer, K., and Klein, M. P. (1993) *Science 260*, 675−678.
6. Britt, R. D., Peloquin, J. M., and Campbell, K. A. (2000) *Annu. Rev. Biophys. Biomol. Struct. 29*, 463−495.
7. Nakamoto, K. (1997) *Infrared and Raman Spectra of Inorganic and Coordination Compounds*, 5th ed., Wiley, New York.
8. Chu, H.-A., Hillier, W., Law, N. A., and Babcock, G. T. (2000) *Biochim. Biophys. Acta* (in press).
9. Chu, H.-A., Gardner, M. T., O'Brien, J. P., Barlow, J., and Babcock, G. T. (1998) in *Photosynthesis: Mechanisms and Effects* (Garab, G., Ed.) pp 1303−1306, Kluwer Academic Publishers, Dordrecht, The Netherlands.
10. Chu, H.-A., Gardner, M. T., O'Brien, J. P., and Babcock, G. T. (1999) *Biochemistry 38*, 4533−4541.
11. Chu, H.-A., Gardner, M. T., Hillier, W., and Babcock, G. T. (2000) *Photosynth. Res.* (in press).
12. Cua, A., Stewart, D. H., Reifler, M. J., Brudvig, G. W., and Bocian, D. F. (2000) *J. Am. Chem. Soc. 122*, 2069−2077.
13. Berthold, D. A., Babcock, G. T., and Yocum, C. F. (1981) *FEBS Lett. 134*, 231−234.
14. Mishra, R. K., and Ghanotakis, D. F. (1994) *Photosynth. Res. 42*, 37−42.

15. Gardner, M. T. (1997) Ph.D. Dissertation, Michigan State University, East Lansing, MI.
16. Hawkins, G. J., Hunneman, R., Gardner, M. T., and Babcock, G. T. (1998) *Infrared Phys. Technol. 39*, 297−306.
17. Noguchi, T., Ono, T., and Inoue, Y. (1995) *Biochim. Biophys. Acta 1228*, 189−200.
18. Dave, B. C., and Czernuszewicz, R. S. (1994) *Inorg. Chim. Acta 227*, 33−41.
19. Holland, P. L., Cramer, C. J., Wilkinson, E. C., Mahapatra, S., Rodgers, K. R., Itoh, S., Taki, M., Fukuzumi, S., Que, L., and Tolman, W. B. (2000) *J. Am. Chem. Soc. 122*, 792−802.
20. Cooper, S. R., and Calvin, M. (1977) *J. Am. Chem. Soc. 99*, 6623−6630.
21. Pecoraro, V. L., and Hsieh, W.-Y. (2000) *Met. Ions Biol. Syst. 37*, 429−504.
22. Sheats, J. E., Czernuszewicz, R. S., Dismukes, G. C., Rheingold, A. L., Petrouleas, V., Stubbe, J., Armstrong, W. H., Beer, R. H., and Lippard, S. J. (1987) *J. Am. Chem. Soc. 109*, 1435−1444.
23. Sanders-Loehr, J., Wheeler, W. D., Shiemke, A. K., Averill, B. A., and Loehr, T. M. (1989) *J. Am. Chem. Soc. 111*, 8084−8093.
24. Yachandra, V. K., Sauer, K., and Klein, M. P. (1996) *Chem. Rev. 96*, 2927−2950.
25. Hasegawa, K., Ono, T., Inoue, Y., and Kusunoki, M. (1999) *Bull. Chem. Soc. Jpn. 72*, 1013−1023.
26. Ruettinger, W. F., Baesjou, P. J., Ho, D. M., Carrell, T. G., Czernuszewicz, D., Ji, R., and Dismukes, G. C. (1999) *J. Inorg. Biochem. 74*, 73.
27. Smith, J. C., Gonzalez-Vergara, E., and Vincent, J. B. (1997) *Inorg. Chim. Acta 255*, 99−103.
28. Thorp, H. H., and Brudvig, G. W. (1991) *New J. Chem. 15*, 479−490.
29. Noguchi, T., Inoue, Y., and Tang, X.-S. (1997) *Biochemistry 36*, 14705−14711.
30. Hoganson, C. W., and Babcock, G. T. (1997) *Science 277*, 1953−1956.
31. Tommos, C., and Babcock, G. T. (1998) *Acc. Chem. Res. 31*, 18−25.
32. Riggs-Gelasco, P. J., Mei, R., Ghanothakis, C. F., Yocum, C. F., and Penner-Hahn, J. E. (1996) *J. Am. Chem. Soc. 118*, 2400−2410.
33. Boussac, A., and Rutherford, A. W. (1988) *Chem. Scr. 28A*, 123−126.
34. Boussac, A., and Rutherford, A. W. (1988) *Biochemistry 27*, 3476−3483.
35. Latimer, M. J., Derose, V. J., Mukerji, I., Yachandra, V. K., Sauer, K., and Klein, M. P. (1995) *Biochemistry 34*, 10898−10909.
36. Cinco, R. M., Robblee, J. H., Rompel, A., Fernandez, C., Yachandra, V. K., Sauer, K., and Klein, M. P. (1998) *J. Phys. Chem. B 102*, 8248−8256.
37. MacLachlan, D. J., Hallahan, B. J., Ruffle, S. V., Nugent, J. H. A., Evans, M. C. W., Strange, R. W., and Hasnain, S. S. (1992) *Biochem. J. 285*, 569−576.
38. Matysik, J., Nachtegaal, G., van Gorkom, H. J., Hoff, A. J., and de Groot, H. J. M. (2000) *Biochemistry 39*, 6751−6755.
39. Law, N. A., Caudle, M. T., and Pecoraro, V. L. (1999) *Adv. Inorg. Chem. 46*, 305−440.
40. Siegbahn, P. E. M. (2000) *Inorg. Chem. 39*, 2923−2935.
41. Limburg, J., Szalai, V. A., and Brudvig, G. W. (1999) *J. Chem. Soc., Dalton Trans.*, 1353−1361.
42. Hillier, W., and Wydrzynski, T. (2000) *Biochemistry 39*, 4399−4405.
43. Noguchi, T., and Sugiura, M. (2000) *Biochemistry 39*, 10943−10949.
44. Falk, M., Huang, C.-H., and Knop, O. (1975) *Can. J. Chem. 53*, 51−57.

BI001751G